IEEE Access
Multidisciplinary | Rapid Review | Open Access Journal

Received July 10, 2019, accepted August 8, 2019, date of publication August 22, 2019, date of current version September 6, 2019.

Digital Object Identifier 10.1109/ACCESS.2019.2936840

Performance Evaluation of Generalized Frequency Division Multiplexing Systems Over Non-Linearities With Memory

ALEXANDER HILARIO-TACURI[1], JOSE MAURO P. FORTES[2], RAIMUNDO SAMPAIO-NETO[2], LEONEL SONCCO[1], DIEGO DONAIRES[1], AND JUAN BORJA[1]

[1]Department of Electronic Engineering, Universidad Nacional de San Agustín de Arequipa, Arequipa 04000, Perú
[2]Department of Electrical Engineering, Pontificia Universidade Católica do Rio de Janeiro, Rio de Janeiro 22451-900, Brazil

Corresponding author: Alexander Hilario-Tacuri (ahilariot@unsa.edu.pe)

This work was derived from the research project funded by the Universidad Nacional de San Agustín de Arequipa under Contract No IBAIB-05-2019-UNSA.

ABSTRACT The fifth generation (5G) of mobile communications systems plans to support different types of applications, where each of these applications may have different requirements. For this reason, the main characteristic of 5G mobile communications systems is the flexibility of their architecture. An interesting proposal that can meet the requirements of these applications is the multi-carrier waveform Generalized Frequency Division Multiplexing (GFDM). However, due to its multi-carrier nature, this new waveform is highly sensitive to non-linear distortions arising mainly from high-power amplifiers (HPA). In addition, the wideband characteristics of multi-carrier signals result in frequency-dependent distortions, typically know as memory effects. This paper presents the development of closed-form analytical expressions that could be used to evaluate the impact of the distortions induced by non-linearities with memory in the out-of-band emissions and the bit error rate performance of GFDM-based systems. The resulting analytical expressions are general enough to obtain numerical results for different parameters of the GFDM-based system.

INDEX TERMS 5G mobile communication, bit error rate, GFDM, non-linear distortion, out-of-band emission, performance analysis, spectral analysis.

I. INTRODUCTION

The main feature in the evolution of mobile communication systems was the progressive increase of the transmission data rate. Unlike its predecessors, it is expected that the next generation of mobile communication systems (5G systems) will have the flexibility of its architecture as main feature, mainly due to the fact that it is expected that diverse applications can be implemented over these communication systems. Some of these applications are: Tactile Internet [1], Machine Type Communications [2], Cognitive Radio [3], Industrial Automation [4], and Autonomous Vehicles [5]. The flexibility of the 5G mobile communication systems is required because in addition to a high data rate, each of these applications has different requirements that may include: ultra low latency, long battery life, low out-of-band emission among others.

The associate editor coordinating the review of this article and approving it for publication was Abbas Jamalipour.

Proposals to meet the requirements of 5G systems that can be found in literature include: Massive MIMO systems [6], mmWave systems [7] and new waveforms [8]. Although many new waveforms have been proposed in recent years [8], [9], many researchers around the world considers (mainly because of their flexibility) that the most promising waveform is the Generalized Frequency Division Multiplexing (GFDM). GFDM is a non-orthogonal multi-carrier waveform that transmit a data block composed of M sub-symbols and N sub-carrier which are cyclic filtered by a shaping pulse that is shifted into frequency and time domains [10]. Studies on GFDM that can be found in the literature include: Bit Error Rate (BER) analysis in different scenarios [11]–[13], spectral analysis [14]–[16], receiver and filter design [17]–[19], interference mitigation [20], [21], practical implementation [22], [23] among others. Despite the great advantages of this new waveform, due to its multi-carrier nature, the GFDM is highly sensitive to

non-linear distortions arising mainly from high-power amplifiers (HPA). Due to all modern communication systems use HPAs, the studies that analyze the performance degradation caused by non-linear distortions in GFDM-based systems are very important. Nevertheless, only a few studies about this research topic can be found in literature [24]–[26]. These studies presents results on the performance of GFDM-based systems in terms of spectral efficiency and bit error rate, obtained by computer simulations and restricted to memory-less non-linear systems.

Unlike the previously mentioned studies, this paper presents the development of closed-form analytical expressions that could be used in the spectral and bit error rate performance analysis of GFDM-based systems operating over non-linear systems with memory. These non-linear systems with memory, are defined using the Wiener-Hammerstein model. The rest of the paper is organized as follows. Section II presents the considered GFDM signal and the model of the non-linear system with memory. Section III shows the development of mathematical expressions to be used for spectral and bit error rate analysis of GFDM-based systems operating over non-linear systems with memory. Numerical results obtained using these mathematical expressions are presented in Section IV and finally, in Section V some conclusions are drawn.

II. SYSTEM MODEL

A. GFDM SIGNAL

The low-pass equivalent of the GFDM signal can be described by [14], [27]

$$\tilde{x}(t) = \sum_{k=-\infty}^{\infty} \tilde{x}_k(t - kT) \tag{1}$$

with $\tilde{x}_k(t)$ representing the GFDM symbol written as

$$\tilde{x}_k(t) = \sum_{n=0}^{N-1} \sum_{m=0}^{M-1} X_{k,n,m} \quad g_m(t) e^{\frac{j2\pi nt}{T_s}} \tag{2}$$

where $X_{k,n,m}$ denotes the m-th complex sub-symbol transmitted over the n-th subcarrier in the k-th time interval, N the number of sub-carriers, M the number of sub-symbols, T_s the sub-symbol duration, $T = MT_s$ the GFDM symbol duration and $g_m(t)$ the shaping pulse, defined as

$$g_m(t) = w_T(t) g(t - mT_s), \tag{3}$$

with $w_T(t)$ being a windowing pulse of duration T and $g(t)$ denoting a periodic pulse with period T.

1) POWER SPECTRAL DENSITY

The auto-correlation function (ACF) of the GFDM signal, described by

$$R_{\tilde{x}}(t, \tau) = E[\tilde{x}(t + \tau)\tilde{x}^*(t)], \tag{4}$$

is given by

$$R_{\tilde{x}}(t, \tau) = \sum_{k_1,n_1,m_1} \sum_{k_2,n_2,m_2} E[X_{k_1,n_1,m_1} X^*_{k_2,n_2,m_2}] \times g_{m_1}(t + \tau - kT) g^*_{m_2}(t - kT) e^{j\frac{2\pi[(n_1 - n_2)t + n_1\tau]}{T_s}}. \tag{5}$$

Considering that, for different subcarriers and time intervals, sub-symbols $X_{k,n,m}$ are statistically independent, that is,

$$E[X_{k_1,n_1,m_1} X^*_{k_2,n_2,m_2}] = \begin{cases} E_X; & (k_1, n_1, m_1) = (k_2, n_2, m_2) \\ 0; & (k_1, n_1, m_1) \neq (k_2, n_2, m_2) \end{cases} \tag{6}$$

it is possible to rewrite (5) as

$$R_{\tilde{x}}(t, \tau) = E_X \sum_{k=-\infty}^{\infty} \sum_{n=0}^{N-1} \sum_{m=0}^{M-1} g_m(t + \tau - kT) g^*_m(t - kT) e^{\frac{j2\pi n\tau}{T_s}} \tag{7}$$

where E_X denote the mean energy of sub-symbols $X_{k,n,m}$. Due to the ACF of the GFDM signal is periodic in time with period T, the mean of the ACF is defined as

$$\bar{R}_{\tilde{x}}(\tau) = \frac{1}{T} \int_T R_{\tilde{x}}(t, \tau) dt. \tag{8}$$

From (7) and (8) and after some mathematical manipulations is possible to write

$$\bar{R}_{\tilde{x}}(\tau) = \frac{E_X}{T} \sum_{n=0}^{N-1} \sum_{m=0}^{M-1} p_m(\tau) e^{\frac{j2\pi n\tau}{T_s}} \tag{9}$$

where $p_m(\tau) = g_m(\tau) * g^*_m(-\tau)$ with "$*$" representing the convolution operation. Finally, the power spectral density of the GFDM signal is given by the Fourier transform of $\bar{R}_{\tilde{x}}(\tau)$, meaning that,

$$S_{\tilde{x}}(f) = \frac{E_X}{T} \sum_{n=0}^{N-1} \sum_{m=0}^{M-1} P_m\left(f - \frac{n}{T_s}\right) \tag{10}$$

where $P_m(\cdot)$ denote the Fourier transform of $p_m(\cdot)$. Considering the definition of $p_m(\tau)$, is possible to rewrite (10) as

$$S_{\tilde{x}}(f) = \frac{E_X}{T} \sum_{n=0}^{N-1} \sum_{m=0}^{M-1} \left| G_m\left(f - \frac{n}{T_s}\right) \right|^2 \tag{11}$$

with $G_m(f)$ representing the Fourier transform of $g_m(t)$.

- General expression for $G_m(f)$: Considering (3), is possible to define $G_m(f)$ as

$$G_m(f) = [W_T(f)] * \left[G(f) e^{-j2\pi mT_s f} \right] \tag{12}$$

with $W_T(f)$ and $G(f)$ representing the Fourier transform of $w_T(t)$ and $g(t)$ respectively. Since $g(t)$ is a periodic pulse of period T, its Fourier transform is given by

$$G(f) = \frac{1}{T} \sum_{i=-\infty}^{\infty} G_T(i/T) \delta(f - i/T) \tag{13}$$

where $G_T(\cdot)$ denote the Fourier transform of the truncated version (in a period T) of $g(t)$. After some mathematical manipulation, is possible to rewrite (12) as

$$G_m(f) = \int_{-\infty}^{\infty} G(\alpha) e^{-j2\pi mT_s \alpha} W_T(f - \alpha) d\alpha \tag{14}$$

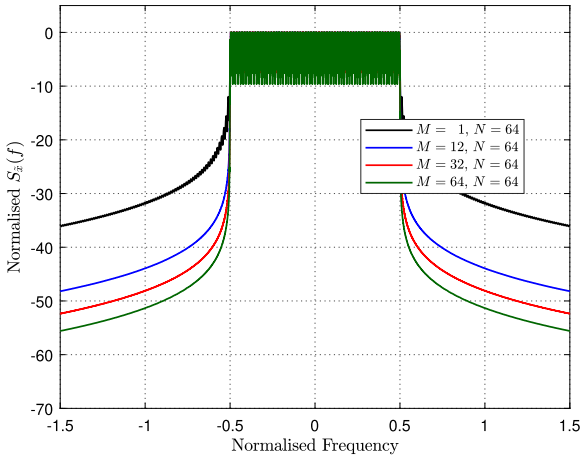

FIGURE 1. Power Spectral density of GFDM signals with $N = 64$ and different M values.

or, by substituting (13) into (14),

$$G_m(f) = \frac{1}{T}\sum_{i=-\infty}^{\infty} G_T(i/T)W_T(f - i/T)e^{-j2\pi mi/M}. \tag{15}$$

In order to demonstrate the use of the previously developed mathematical expressions, Fig. 1 shows power spectral density curves for GFDM signals considering different values of M. In this figure it was also considered that $T_s = 1\mu$s, $N = 64$, $w_T(t)$ is a rectangular pulse and $g(t)$ is a raised cosine shaping pulse.

B. NON-LINEAR SYSTEM WITH MEMORY

In this work, the Wiener-Hammerstein model is used to characterize the non-linear system with memory. As can be seen in Fig. 2, two linear time-invariant systems (with impulse responses $\tilde{u}(t)$ and $\tilde{h}(t)$) are used to consider the memory effects of the non-linear system.

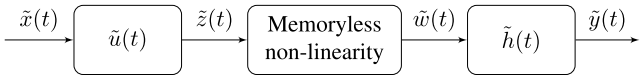

FIGURE 2. Block diagram of the Wiener-Hammerstein model.

The memoryless non-linearity in Fig. 2 is assumed to be of polynomial type [28], that is,

$$\tilde{w}(t) = \sum_{\ell=0}^{L} \gamma_{2\ell+1}\tilde{z}^{\ell+1}(t)\tilde{z}^{*\ell}(t). \tag{16}$$

with L denoting the maximum odd order of the non-linearity and $\gamma_{2\ell+1}$ the coefficients used for modeling the non-linearity.

Note that, the relationship between the input and output signals of the non-linear system presented in Fig.2 can also be modeled using the Volterra series [29], that is,

$$\tilde{y}(t) = \sum_{\ell=0}^{L}\int_{-\infty}^{\infty}\cdots\int_{-\infty}^{\infty}\tilde{k}_{2\ell+1}(\alpha_1,\ldots,\alpha_{2\ell+1})\prod_{r=1}^{\ell+1}\tilde{x}(t-\alpha_r) \times\prod_{s=\ell+2}^{2\ell+1}\tilde{x}^*(t-\alpha_s)d\alpha_1,\ldots,d\alpha_{2\ell+1} \tag{17}$$

with $\tilde{k}_{2\ell+1}(\alpha_1,\ldots,\alpha_{2\ell+1})$ denoting the Volterra kernels defined by

$$\tilde{k}_{2\ell+1}(\alpha_1,\ldots,\alpha_{2\ell+1}) = \gamma_{2\ell+1}\int_{-\infty}^{\infty}\tilde{h}(v)\prod_{r=1}^{\ell+1}\tilde{u}(\alpha_r - v) \times\prod_{s=\ell+2}^{2\ell+1}\tilde{u}^*(\alpha_s - v)dv \tag{18}$$

III. PERFORMANCE EVALUATION

A. SPECTRAL ANALYSIS: OUT-OF-BAND EMISSIONS

The Price's Theorem for complex values [14], [30], states that the relationship between the ACFs of inputs and output signals of a memory-less non-linear system is given by

$$\frac{\partial R_{\tilde{w}}(\tau)}{\partial R_{\tilde{z}}(\tau)} = E\left[\frac{\partial^2 w(t)w^*(t+\tau)}{\partial\tilde{z}(t)\partial\tilde{z}^*(t+\tau)}\right]. \tag{19}$$

Considering (16), is possible to rewrite (19) as

$$\frac{\partial R_{\tilde{w}}(\tau)}{\partial R_{\tilde{z}}(\tau)} = \sum_{\ell_1=0}^{L}\sum_{\ell_2=0}^{L}\gamma_{2\ell_1+1}\gamma^*_{2\ell_2+1}(\ell_1+1)(\ell_2+1) \times E\left[\tilde{z}^{\ell_1}(t+\tau)\tilde{z}^{*\ell_1}(t+\tau)\tilde{z}^{\ell_2}(t)\tilde{z}^{*\ell_2}(t)\right]. \tag{20}$$

The expected value in (20) can be computed using the Reed's Theorem [31]. Note that, using (20), is posible to compute the ACF of the memory-less non-linear output signal, for instance, if a third order non-linearity is considered (meaning that $L = 1$), the ACF of $\tilde{w}(t)$ is defined by

$$R_{\tilde{w}}(\tau) = C_1 R_{\tilde{z}}(\tau) + C_3 R^*_{\tilde{z}}(\tau)R^2_{\tilde{z}}(\tau) \tag{21}$$

where $R_{\tilde{z}}(\tau)$ represent the ACF of $\tilde{z}(t)$ and the complex coefficients C_1 and C_3 are given by

$$C_1 = |\gamma_1 + 2\gamma_3 P_{\tilde{z}}|^2 \tag{22}$$

and

$$C_3 = 2|\gamma_3|^2 \tag{23}$$

respectively. In (22), $P_{\tilde{z}}$ represent the mean power of $\tilde{z}(t)$ and can be computed using

$$P_{\tilde{z}} = R_{\tilde{z}}(0). \tag{24}$$

The power spectral density of $\tilde{w}(t)$ is then obtained applying the Fourier transform to $R_{\tilde{w}}(\tau)$, thus,

$$S_{\tilde{w}}(f) = C_1 S_{\tilde{z}}(f) + C_3 S^*_{\tilde{z}}(-f) * S_{\tilde{z}}(f) * S_{\tilde{z}}(f) \tag{25}$$

with $S_{\tilde{z}}(f)$ representing the power spectral density of $\tilde{z}(t)$ given by

$$S_{\tilde{z}}(f) = |\tilde{U}(f)|^2 S_{\tilde{x}}(f). \tag{26}$$

Finally, the power spectral density of the non-linear output $\tilde{y}(t)$ can be obtained using

$$S_{\tilde{y}}(f) = |\tilde{H}(f)|^2 S_{\tilde{w}}(f). \tag{27}$$

In (26) and (27), $\tilde{U}(f)$ and $\tilde{H}(f)$ denote the Fourier transform of $\tilde{u}(t)$ and $\tilde{h}(t)$ respectively.

In this work, the spectral analysis is quantified according to the out-of-band emissions (*OOB*) of the GFDM signal. The *OOB* is defined as the ratio between the energy that is inside and outside a certain allocated bandwidth B [14], [32].

$$OOB_e = \frac{\int_{f \notin B} S_{\tilde{y}}(f)df}{\int_{f \in B} S_{\tilde{y}}(f)df} \tag{28}$$

B. BIT ERROR RATE

According to the Bussgang's Theorem [33], in any time interval the relationship between the input and output signal of a memoryless non-linear channel is defined as

$$\tilde{w}_k(t) = \alpha \tilde{z}_k(t) + \tilde{b}_k(t) \tag{29}$$

where α is a complex coefficient that, for a third-order memoryless non-linearity of polynomial type, is given by

$$\alpha = \gamma_1 + 2\gamma_3 P_{\tilde{z}} \tag{30}$$

and $b_k(t)$ represent a zero mean non-linear noise uncorrelated of $\tilde{z}_k(t)$. For a larger number of subcarriers this non-linear noise can be approximated by a random Gaussian process. The received signal distorted by the non-linear channel and corrupted by an additive white Gaussian noise (AWGN), with power spectral density N_0, is given by

$$\tilde{r}_k(t) = \tilde{y}_k(t) + \tilde{n}(t) \tag{31}$$

where the non-linear distorted output $\tilde{y}_k(t)$ can be write as

$$\tilde{y}_k(t) = \alpha \tilde{x}_k(t) * \tilde{u}(t) * \tilde{h}(t) + \tilde{b}_k(t) * \tilde{h}(t). \tag{32}$$

To obtain analytical expressions for the bit error rate of GFDM systems, matched filters are considered in the receiver as shown in Fig. 3. According to this block diagram, the m-th complex sub-symbol received on the n-th subcarrier in the k-th time interval is given by

$$\hat{X}_{k,n,m} = \int_{-\infty}^{\infty} \tilde{r}_k(t) g_m^*(t) e^{\frac{-j2\pi nt}{T_s}} dt. \tag{33}$$

By using (2), (32) and (31) it is possible to rewrite (33) as

$$\hat{X}_{k,n,m} = R_{n,m} X_{k,n,m} + I_{k,n,m} + B_{k,n,m} + N_{k,n,m} \tag{34}$$

where $I_{k,n,m}$ represents the self-interference of the GFDM symbol given by

$$I_{k,n,m} = \sum_{\substack{n_1=0 \\ (n_1 \neq n,\, m_1 \neq m)}}^{N-1} \sum_{m_1=0}^{M-1} X_{k,n_1,m_1} R_{n_1,m_1}^{(n,m)}, \tag{35}$$

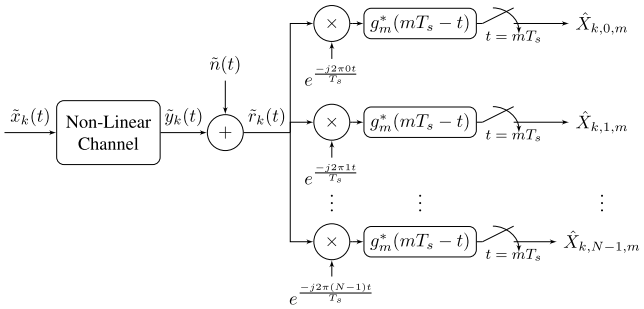

FIGURE 3. Matched filter receiver for GFDM systems.

with $R_{n_1,m_1}^{(n,m)}$ defined as

$$R_{n_1,m_1}^{(n,m)} = \alpha \int_{-\infty}^{\infty} G_{m_1}\left(f - \frac{n_1}{T_s}\right) G_m^*\left(f - \frac{n}{T_s}\right) \tilde{U}(f)\tilde{H}(f)df. \tag{36}$$

Still in (34), $B_{k,n,m}$ denotes the term due to the non-linear noise given by

$$B_{k,n,m} = \int_{-\infty}^{\infty}\int_{-\infty}^{\infty} \tilde{b}_k(t)\tilde{H}(f) G_m^*\left(f - \frac{n}{T_s}\right) e^{-j2\pi ft} dtdf, \tag{37}$$

$N_{k,n,m}$ represents the term due to AWGN given by

$$N_{k,n,m} = \int_{-\infty}^{\infty} \tilde{n}(t) g_m^*(t) e^{\frac{-j2\pi nt}{T_s}} dt \tag{38}$$

and $R_{n,m}$ represents a particular case of $R_{n_1,m_1}^{(n,m)}$ where $(n_1, m_1 = n, m)$, that is,

$$R_{n,m} = \alpha \int_{-\infty}^{\infty} \left| G_m(f - \frac{n}{T_s}) \right|^2 \tilde{U}(f)\tilde{H}(f)df. \tag{39}$$

- Characterization of $I_{k,n,m}$: From (35) and using the Central Limit Theorem, it is possible to approximate the self-interference $I_{k,n,m}$ (for larger values of M and N) by a gaussian random variable with zero mean and variance

$$Var[I_{k,n,m}] = \sum_{\substack{n_1=0 \\ (n_1 \neq n,\, m_1 \neq m)}}^{N-1} \sum_{m_1=0}^{M-1} |R_{n_1,m_1}^{(n,m)}|^2. \tag{40}$$

- Characterization of $B_{k,n,m}$: From (37) and considering the statistical characteristics of $\tilde{b}_k(t)$, it can be shown that $B_{k,n,m}$ is a gaussian random variable with zero mean and variance given by

$$Var[B_{k,n,m}] = \int_{-\infty}^{\infty} S_{\tilde{b}_k}(f)|\tilde{H}(f)|^2 \left| G_m\left(f - \frac{n}{T_s}\right) \right|^2 df \tag{41}$$

with $S_{\tilde{b}_k}(f)$ denoting the power spectral density of $\tilde{b}_k(t)$. For a third-order memoryless non-linearity of polynomial type, $S_{\tilde{b}_k}(f)$ is given by

$$S_{\tilde{b}_k}(f) = C_3 S^*_{\tilde{z}}(-f) * S_{\tilde{z}}(f) * S_{\tilde{z}}(f). \tag{42}$$

- Characterization of $N_{k,n,m}$: From (38) and considering the statistical characteristics of the AWGN, $\tilde{n}(t)$, it results that $N_{k,n,m}$ is a gaussian random variable with zero mean and variance $\sigma^2_{N_{n,m}} = N_0\, R_{n,m}$.

Assuming that the GFDM receiver has a perfect knowledge of $R_{n,m}$, the decision can be made based on the variable

$$D_{k,n,m} = \frac{\hat{X}_{k,n,m}}{R_{n,m}} = X_{k,n,m} + Z_{k,n,m}, \tag{43}$$

where

$$Z_{k,n,m} = \frac{I_{k,n,m}}{R_{n,m}} + \frac{B_{k,n,m}}{R_{n,m}} + \frac{N_{k,n,m}}{R_{n,m}} \tag{44}$$

is a zero mean gaussian random variable with variance

$$\sigma^2_{Z_{n,m}} = \frac{Var[I_{k,n,m}]}{|R_{n,m}|^2} + \frac{Var[B_{k,n,m}]}{|R_{n,m}|^2} + \frac{\sigma^2_{N_{n,m}}}{|R_{n,m}|^2}. \tag{45}$$

The approximated bit error rate (BER) for each subsymbol and subcarrier of a GFDM system using a $\mathcal{M}$-PSK modulation is given by

$$P_b(n,m) \simeq 2Q\left(\sqrt{2\,\mathrm{SNR}(n,m)}\sin\left(\frac{\pi}{\mathcal{M}}\right)\right) \tag{46}$$

where $Q(\cdot)$ is the well-known Q-function defined by [34]

$$Q(x) = \frac{1}{\sqrt{2\pi}}\int_x^\infty e^{-\alpha^2/2} d\alpha \tag{47}$$

and

$$\mathrm{SNR}(n,m) = \frac{E_X}{\sigma^2_{Z_{n,m}}}. \tag{48}$$

Finally, the average BER can be computed by

$$\bar{P}_b = \frac{1}{N\,M}\sum_{n=0}^{N-1}\sum_{m=0}^{M-1} P_b(n,m). \tag{49}$$

IV. NUMERICAL RESULTS

In this section, the mathematical expressions previously developed are used to evaluate the performance of a particular GFDM systems using BPSK modulation with sub-symbol duration $T_s = 1\mu$s. In this particular case, is also considered that $w_T(t)$ is a rectangular windowing pulse and $g(t)$ is raised cosine shaping pulse, periodic with period T, meaning that, the truncated version of $g(t)$ is given by

$$g_T(t) = \mathrm{sinc}(\pi t/T_s)\frac{\cos(\pi\beta t/T_s)}{1-(2\beta t/T_s)^2}. \quad t \in \left[-\frac{T}{2}, \frac{T}{2}\right] \tag{50}$$

where β denotes the roll-off factor of the raised cosine shaping pulse. The non-linear system is considered of third order with complex coefficients $\gamma_1 = 1$ and $\gamma_3 = -0.25$ [14] and the frequency response of the two linear time-invariant systems are given by

$$\tilde{U}(f) = \tilde{G}(f) = \frac{1}{1+j\frac{2f}{B_0}} \tag{51}$$

where B_0 denotes the 3dB bandwidth. Results were obtained for different values of Input Back-Off (IBO), defined as

$$\mathrm{IBO} = 10\log_{10}\left(\frac{P_{sat}}{P_{in}}\right) \tag{52}$$

with P_{sat} and P_{in} being the saturation and average input power, respectively.

A. OUT-OF-BAND EMISSIONS

Figs. 4 and 5 shows the power spectral density of the non-linear distorted GFDM signal for different values of the parameters N and M and considering IBO $=$ 4 dB and $\beta = 0.5$. At this point, is good to point out that these figures were obtained using only (11), (25), (26) and (27). All these figures, also shows the power spectral density of the input GFDM signal with the same parameters.

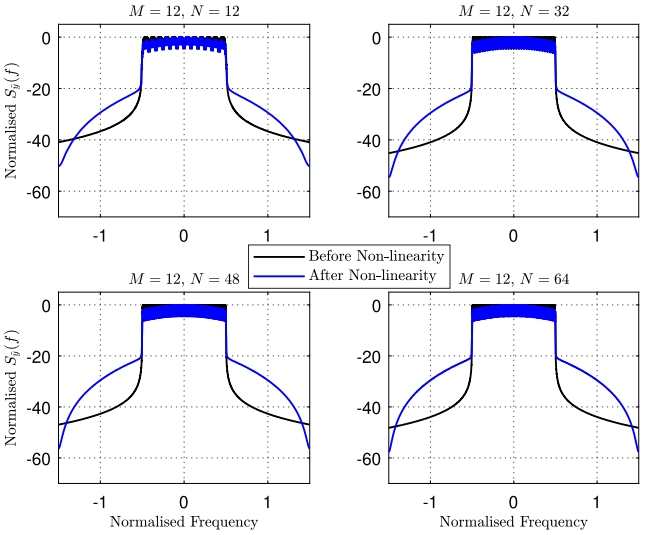

FIGURE 4. Power Spectral density of the non-linear distorted GFDM signal for $M = 12$ and different N values.

Fig. 4 shows the power spectral density for a GFDM signal with a specific number of subsymbols ($M = 12$) and for different numbers of subcarriers ($N = 12, 32, 48, 64$). As can be seen in these figures, the larger the value of N, the lower the out-of-band emissions of the non-linear distorted signal. Analogously, Fig. 5 illustrate the power spectral density for a GFDM signal with a specific number of subcarriers ($N = 64$) and for different numbers of subsymbols ($M = 1, 12, 32, 64$). Again, from this figure it is possible to conclude that, the larger the value of M, the lower the out-of-band emissions of the non-linear distorted GFDM signal. Note that, the exact values of the OOB emissions can be computed using (27) and, for the specific values considered in this section, they are listed in Table 1.

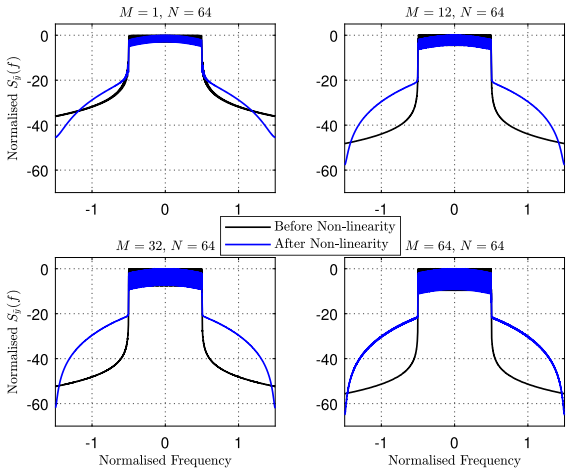

FIGURE 5. Power Spectral density of the non-linear distorted GFDM signal for $N = 64$ and different M values.

TABLE 1. Out-of-band emission for different values of M and N.

N \ M	1	12	32	64
12	0.0052	0.0024	0.0022	0.0021
32	0.0034	0.0020	0.0019	0.0018
48	0.0030	0.0019	0.0018	0.0018
64	0.0027	0.0018	0.0018	0.0017

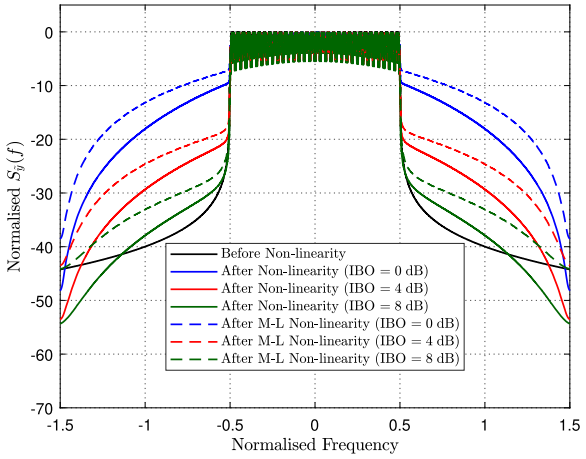

FIGURE 6. Power Spectral density of the non-linear distorted GFDM signal for different values of IBO.

Fig. 6 shows the power spectral density of the non-linear distorted GFDM signal with $\beta = 0.5$, $M = 12$, $N = 32$ and for different values of IBO. In order to demonstrate the robustness and flexibility of the develop analytical expressions, this figure also shows the power spectral density of a GFDM signal distorted by a memory-less non-linear system with the same parameters. As expected, this figure confirms that the larger the IBO value, the lower the out-of-band emission of the non-linear distorted GFDM signal. The exact values of these emissions are listed in Table 2.

TABLE 2. Out-of-band emission for different IBO values.

NL \ IBO	0 dB	4 dB	8 dB
With memory	0.0237	0.0022	0.0006
Memory-less	0.0447	0.0039	0.0010

B. BIT ERROR RATE

To obtain the BER of GFDM-based systems (46), (48) and (49) were used. For comparison purposes, Figs. 7 to 10 show BER curves corresponding to GFDM-based systems corrupted by AWGN and non-linearities and BER curves of GFDM-based systems corrupted only by AWGN. The effect of the total number of subcarriers N on the BER of a GFDM-based system with IBO $= 4$ dB and $\beta = 0.5$ is illustrated in Fig. 7. This figure indicates that the BER varies very little with N, for both situations considered AWGN with and without a non-linear system with memory.

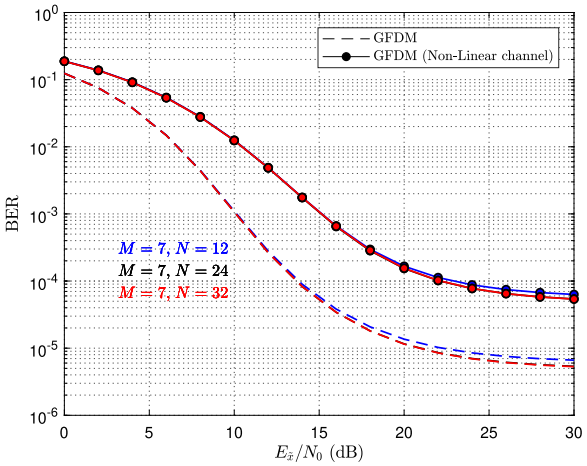

FIGURE 7. BER of a GFDM-based system for different N values.

To illustrate the effects of the total number of sub-symbols M, Fig. 8 shows the BER curves for a GFDM-based system with IBO $= 4$ dB, $\beta = 0.5$ and for different values of M. This figure confirms that, the larger the value of M the worse is the performance of the GFDM system. Note that, the curve for $m = 1$ also represent the BER of a classical OFDM system and as can be seen in Fig 8, it has the worst BER performance.

The effect of the shaping pulse on the BER of GFDM-based systems with IBO $= 4$ dB, $M = 7$, $N = 64$ and for different values of β can be visualised in Fig. 9. This figure shows that, the larger the value of β, the worse the performance of the system.

Finally, to illustrate the effects of the non-linear system with memory, Fig. 10 presents the BER of GFDM-based systems with $M = 7$, $N = 64$, $\beta = 0.5$ and for different values of IBO. This figure confirms that the closer to the linear region the non-linear channel operates, the better is the performance of the system.

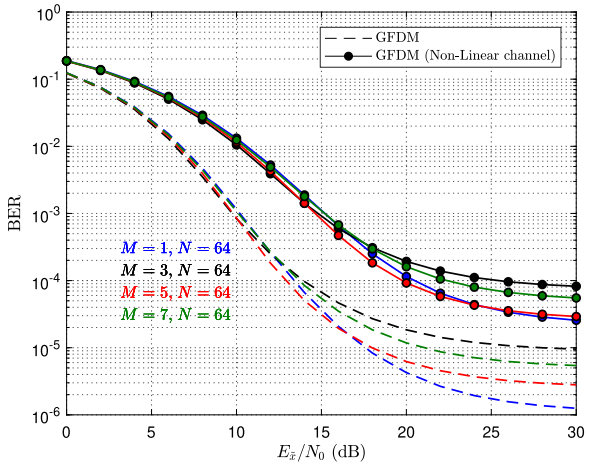

FIGURE 8. BER of a GFDM-based system for different M values.

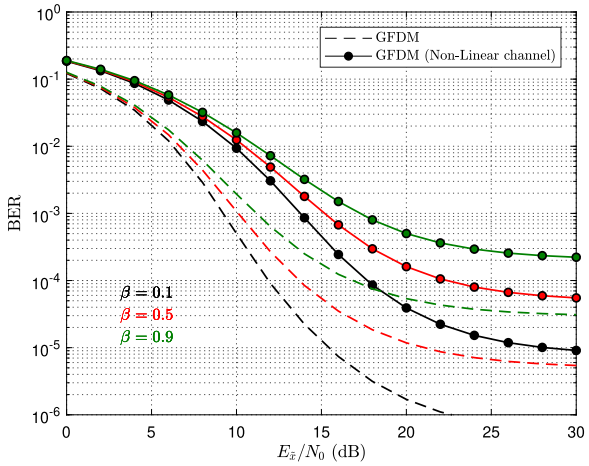

FIGURE 9. BER of a GFDM signal for different values of β.

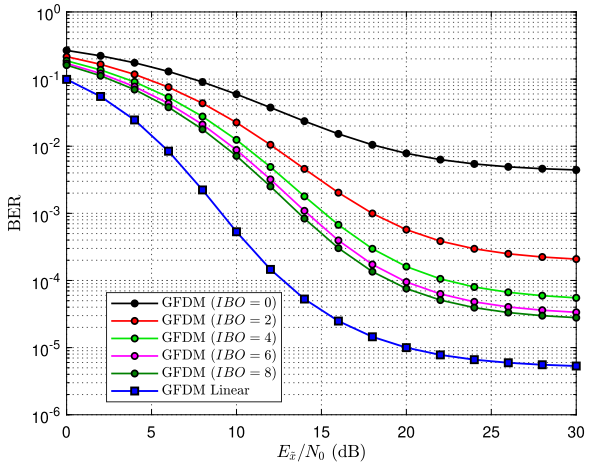

FIGURE 10. BER of a GFDM signal for different values of the IBO.

V. CONCLUSION

This paper presented the development of closed-form analytical expressions that can be used to evaluate the performance of GFDM-based systems operating over non-linear systems with memory. The considered performance metrics were the out-of-band emissions and the bit error rate. As shown in Figs. 4 to 6 the analytical expressions obtained for the power spectral density of the non-linear distorted GFDM signal are general enough to be used with different parameters of the GFDM-based system and of the non-linearity. In addition, these expressions allow for easily obtained out-of-band emission values. Analogously, as shown in Figs. 7 to 10, the derived analytically expressions for the bit error rate, can easily provide BER performance curves for different parameters of the GFDM-based system and of the non-linearity with memory.

REFERENCES

[1] G. P. Fettweis, "The tactile Internet: Applications and challenges," *IEEE Veh. Technol. Mag.*, vol. 9, no. 1, pp. 64–70, Mar. 2014.
[2] H. Shariatmadari, R. Ratasuk, S. Iraji. A. Laya, T. Taleb, R. Jäntti, and A. Ghosh, "Machine-type communications: Current status and future perspectives toward 5G systems," *IEEE Commun. Mag.*, vol. 53, no. 9, pp. 10–17, Sep. 2015.
[3] S. Haykin, "Cognitive radio: Brain-empowered wireless communications," *IEEE J. Sel. Areas Commun.*, vol. 23, no. 2, pp. 201–220, Feb. 2005.
[4] M. Wollschlaeger, T. Sauter, and J. Jasperneite, "The future of industrial communication: Automation networks in the era of the Internet of Things and industry 4.0," *IEEE Ind. Electron. Mag.*, vol. 11, no. 1, pp. 17–27, Mar. 2017.
[5] C. Campolo, A. Molinaro, A. Iera, and F. Menichella, "5G network slicing for vehicle-to-everything services," *IEEE Wireless Commun.*, vol. 24, no. 6, pp. 38–45, Dec. 2017.
[6] G. Fodor, N. Rajatheva, W. Zirwas, L. Thiele, M. Kurras, K. Guo, A. Tolli, J. H. Sorensen, and E. de Carvalho, "An overview of massive MIMO technology components in METIS," *IEEE Commun. Mag.*, vol. 55, no. 6, pp. 155–161, Jun. 2017.
[7] G. Fodor, N. Rajatheva, W. Zirwas, L. Thiele, M. Kurras, K. Guo, A. Tolli, J. H. Sorensen, and E. de Carvalho, "An overview of massive MIMO technology components in METIS," *IEEE Commun. Mag.*, vol. 56, pp. 137–143, Jun. 2018.
[8] P. Banelli, S. Buzzi, G. Colavolpe, A. Modenini, F. Rusek, and A. Ugolini, "Modulation formats and waveforms for 5G networks: Who will be the heir of OFDM?: An overview of alternative modulation schemes for improved spectral efficiency," *IEEE Signal Process. Mag.*, vol. 31, no. 6, pp. 80–93, Nov. 2014.
[9] R. Gerzaguet, N. Bartzoudis, L. G. Baltar, V. Berg, J.-B. Doré, D. Kténas, O. Font-Bach, X. Mestre, M. Payaró, M. Färber, and K. Roth, "The 5G candidate waveform race: A comparison of complexity and performance," *J. Wireless Commun. Netw.*, vol. 2017, Jan. 2017, Art. no. 13.
[10] G. Fettweis, M. Krondorf, and S. Bittner, "GFDM—Generalized frequency division multiplexing," in *Proc. IEEE 69th Veh. Technol. Conf.*, Jun. 2009, pp. 1–4.
[11] D. Gaspar, L. Mendes, and T. Pimenta, "GFDM BER under synchronization errors," *IEEE Commun. Lett.*, vol. 21, no. 8, pp. 1743–1746, Aug. 2017.
[12] Z. Wang, L. Mei, X. Sha, and V. C. M. Leung, "BER analysis of WFRFT precoded OFDM and GFDM waveforms with an integer time offset," *IEEE Trans. Veh. Technol.*, vol. 67, no. 10, pp. 9097–9111, Oct. 2018.
[13] Z. Wang, L. Mei, and X. Sha, "BER analysis for GFDM systems with Gabor MMSE receiver," *IEEE Commun. Lett.*, vol. 22, no. 11, pp. 2222–2225, Nov. 2018.
[14] A. Hilario-Tacuri, J. M. P. Fortes, and R. Sampaio-Neto, "Analytical spectral evaluation of GFDM systems over non-linear channels with memory," in *Proc. IEEE 10th Latin-Amer. Conf. Commun. (LATINCOM)*, Nov. 2018, pp. 1–5.
[15] D. Zhang, A. Festag, and G. P. Fettweis, "Performance of generalized frequency division multiplexing based physical layer in vehicular communications," *IEEE Trans. Veh. Technol.*, vol. 66, no. 11, pp. 9809–9824, Nov. 2017.
[16] I. Almeida and L. Mendes, "Linear GFDM: A low out-of-band emission configuration for 5G air interface," in *Proc. IEEE 5G World Forum (5GWF)*, Nov. 2018, pp. 311–316.
[17] P.-C. Chen, B. Su, and Y. Huang, "Matrix characterization for GFDM: Low complexity MMSE receivers and optimal filters," *IEEE Trans. Signal Process.*, vol. 65, no. 18, pp. 4940–4955, Sep. 2017.
[18] B. Lim and Y. Ko, "Low-complexity joint-MMSE GFDM receiver," *IEEE Trans. Commun.*, vol. 66, no. 4, pp. 1661–1674, Dec. 2017.

[19] S. Han, Y. Sung, and Y. H. Lee, "Filter design for generalized frequency-division multiplexing," *IEEE Trans. Signal Process.*, vol. 65, no. 7, pp. 1644–1659, Apr. 2017.
[20] S. Tiwari, S. S. Das, and K. K. Bandyopadhyay, "Precoded generalised frequency division multiplexing system to combat inter-carrier interference: Performance analysis," *IET Commun.*, vol. 9, no. 15, pp. 1829–1841, May 2015.
[21] M. Towliat and S. M. J. A. Tabatabaee, "GFDM interference mitigation without noise enhancement," *IEEE Commun. Lett.*, vol. 22, no. 5, pp. 1042–1045, May 2018.
[22] J. Demel, C. Bockelmann, and A. Dekorsy, "Evaluation of a software defined GFDM implementation for industry 4.0 applications," in *Proc. IEEE Int. Conf. Ind. Technol. (ICIT)*, May 2017, pp. 1283–1288.
[23] W. D. Dias, L. L. Mendes, and J. J. P. C. Rodrigues, "Low complexity GFDM receiver for frequency-selective channels," *IEEE Commun. Lett.*, vol. 1, no. 7, pp. 1166–1169, May 2019.
[24] A. Ortega, L. Fabbri, and V. Tralli, "Performance evaluation of GFDM over nonlinear channel," in *Proc. Int. Conf. Inf. Commun. Technol. Converg. (ICTC)*, Dec. 2016, pp. 12–17.
[25] A. E. W. Jayati and T. Suryani, "Analysis of non-linear distortion effect based on Saleh model in GFDM system," in *Proc. IEEE Int. Conf. Commun., Netw. Satellite (Comnetsat)*, Jan. 2018, pp. 1–6.
[26] R. M. Borges, T. R. R. Marins, M. S. B. Cunha, H. R. D. Filgueiras, I. F. da Costa, R. N. da Silva, D. H. Spadoti, L. L. Mendes, and A. C. Sodré, "Integration of a GFDM-based 5G transceiver in a GPON using radio over fiber technology," *J. Lightw. Technol.*, vol. 36, no. 19, pp. 4468–4477, Apr. 2018.
[27] A. Nimr, D. Zhang, A. Martinez, and G. Fettweis, "A study on the physical layer performance of GFDM for high throughput wireless communication," in *Proc. 25th Eur. Signal Process. Conf. (EUSIPCO)*, Oct. 2017, pp. 638–642.
[28] S. Benedetto, E. Biglieri, and V. Castellani, *Digital Transmission Theory*. Upper Saddle River, NJ, USA: Prentice-Hall, 1987.
[29] M. Gerzon, "Volterra series describing the substitution of nonlinear components in nonlinear networks," *IEEE Trans. Circuits Syst.*, vol. CS-23, no. 8, pp. 509–510, Aug. 1976.
[30] A. van den Bos, "Price's theorem for complex variates," *IEEE Trans. Inf. Theory*, vol. 42, no. 1, pp. 286–287, Jan. 1996.
[31] I. S. Reed, "On a moment theorem for complex Gaussian process," *IRE Trans. Inf. Theory*, vol. 8, pp. 194–195, Apr. 1962.
[32] N. Michailow, M. Matthé, I. S. Gaspar, A. N. Caldevilla, L. L. Mendes, A. Festag, and G. Fettweis, "Generalized frequency division multiplexing for 5th generation cellular networks," *IEEE Trans. Commun.*, vol. 62, no. 9, pp. 3045–3061, Sep. 2014.
[33] J. Bussgang, "Cross correlation function of amplitude-distorted Gaussian signals," Res. Lab. Electron., Massachusetts Inst. Technol., Cambridge, Tech. Rep. 216, Mar. 1952.
[34] T. S. Rappaport, *Wireless Communications: Principles and Practice*. Upper Saddle River, NJ, USA: Prentice-Hall, 1999.

ALEXANDER HILARIO-TACURI was born in Perú, in 1988. He received the degree in electronic engineering (telecommunications) from the Universidad Nacional de San Agustín de Arequipa (UNSA), Perú, in 2008, and the M.Sc. and Ph.D. degrees in electrical engineering from the Pontifícia Universidade Católica do Rio de Janeiro (PUC-Rio), Brazil, in 2010 and 2014, respectively. After Ph.D. graduation, he was a Senior Researcher with the Engenho Company on research and development, where he was the Head of the Research Group. From March 2015 to December 2016, he was a Postdoctoral Fellow with the Department of Electrical Engineering, Pontifícia Universidade Católica do Rio Grande do Sul, Porto Alegre, Brazil. From August 2015 to November 2016, he was a Visiting Researcher with Stanford University. He returned to UNSA, in January 2017, and since then, he has been a Professor with the Electronic Engineering Department. In 2018, while on a sabbatical leave, he was a Postdoctoral Fellow with the Department of Electrical Engineering, PUC-Rio, working in the University Center for Telecommunications Studies (CETUC). He has published many articles in national and international journals and conferences. His main research interests include 5G cellular networks, communication theory, satellite communications, estimation theory, digital transmission, and signal processing for communications.

JOSE MAURO P. FORTES was born in Rio de Janeiro, Brazil, in 1950. He received the B.S. and M.Sc. degrees in electrical engineering (telecommunications) from the Pontifícia Universidade Católica do Rio de Janeiro (PUC-Rio), in 1973 and 1976, respectively, and the M.Sc. and Ph.D. degrees in electrical engineering from Stanford University, USA, in 1978 and 1980, respectively. He returned to PUC-Rio, in June 1980, and was a Professor with the Electrical Engineering Department, until 2018, working at the University Center for Telecommunications Studies (CETUC), where he was the Head of the Communication Systems Group, from 2000 to 2018. He is currently an Independent Consultant in satellite communications. In 1992, while on sabbatical leave, he was a Researcher with the General Electric Research and Development Center, Schenectady, USA. He has published several articles in national and international journals and conferences. He has coordinated a number of research projects and has been a Consultant in satellite communications for several private companies and telecommunications agencies. His main research interests include communication theory, satellite communications, estimation theory, and digital transmission. For two terms (from 1996 to 2000), he was the President of the Brazilian Telecommunications Society (an IEEE ComSoc Sister Society), and for 13 years, he was the Vice-Chairman of the ITU-R Study Group 4 (Fixed Satellite Service).

RAIMUNDO SAMPAIO-NETO received the Diploma and M.Sc. degrees from the Pontificia Universidade Católica do Rio de Janeiro (PUC-Rio), Brazil, in 1975 and 1978, respectively, and the Ph.D. degree from the University of Southern California (USC), Los Angeles, in 1983, all in electrical engineering. From November 1983 to June 1984, he was a Postdoctoral Fellow with the Department of Electrical Engineering, Communication Sciences Institute, USC, and a member of the Technical Staff of Axiomatic Corporation, Los Angeles. He is currently a Researcher with the Center for Studies in Telecommunications (CETUC) and an Associate Professor with the Department of Electrical Engineering, PUC-Rio, where he has been affiliated, since July 1984. In 1991, he was a Visiting Professor with the Department of Electrical Engineering, USC. He has participated in various projects and consulted for several private companies and government agencies. His research interests include communication theory, digital transmission, and signal processing for communications, areas in which he has published more than 200 articles in refereed journals and conferences. He has served as a member of its Advisory Council for four terms and as an Associate Editor for the society journal: *Journal of Communication and Information Systems*. He is also an Emerit Member of SBrT. He was a Co-Organizer of the Session on Recent Results for the IEEE Workshop on Information Theory, Salvador, Brazil, 1992. He also served as the Technical Program Co-Chairman for the IEEE Global Telecommunications Conference (Globecom'99), Rio de Janeiro, and as a Technical Program Member of several national and international conferences. He was in the office for three terms on the Board of Directors of the Brazilian Communications Society (SBrT).

LEONEL SONCCO was born in Perú, in 1995. In 2014, he began his studies in electronic engineering at the National University of San Agustín (UNSA). He is currently a part of the top third in the ranking of his school, being in the last year in the career of electronic engineering. He is also a part of the team in the research line in information technologies and communications networks funded by UNSA. His research interests include mobile communication systems, and digital signal processing and applications.

DIEGO DONAIRES was born in Perú, in 1997. In 2015, he began his studies in electronic engineering at the National University of San Agustín (UNSA). He is currently a part of the fifth higher in the ranking of his school, being in the last year in the career of electronic engineering. He is also a part of the team in the research line in information technologies and communications networks funded by UNSA. His research interests include mobile communication systems, and digital signal processing and applications.

JUAN BORJA was born in Arequipa, Perú, in 1951. He graduated as an Electronic Engineer from Ricardo Palma University, Lima, Perú. He received the M.Sc. degree in industrial engineering with a focus on production management and the Ph.D. degree in production engineering from the National University of San Agustín de Arequipa (UNSA), Arequipa, Perú, in 2006 and 2008, respectively. He carried out studies in identification, formulation, and evaluation of public investment projects by the Higher School of Engineering, National University of Engineering, in 2012, and specialization in project management under the PMI approach by the National School of Control, in 2007. He has more than 30 years of work experience in companies in the electricity sector, in the Electric Society of South West of Perú (SEAL), from 1977 to 1994, occupying the position of Head of the Commercial Technical Unit, Communications Unit, and Workshops Department, developing projects for the implementation of radio communications systems, laboratory for the testing of energy meters, in the Electric Generation Company of Arequipa S.A. (EGASA), from 1994 and 2013, holding the position of Head of the Telecommunications and Control Department, where he developed projects for the implementation of telecommunications systems by fiber optics and digital radio-relays by microwaves, and in the EGASA Control Center, where he was involved in the automation of power plants: generation and hydraulic water storage system for the city of Arequipa. He has extensive experience in university teaching at the Ricardo Palma University and UNSA in the specialty courses of telecommunications and project management. He has participated as an Exhibitor in many seminars and conferences on automation issues, control centers, and telecommunications systems. He supported some research projects in the aspects of project management.